scientific reports

Check for updates

OPEN

Glypican 3 as target therapy to prevent cell migration and proliferation in rhabdomyosarcoma

Maira Bacchiega[1,2], Stefania D'Agostino[1,2], Antonella Grigoletto[3], Elena Poli[1,2], Paolo Bonvini[2], Gianni Bisogno[1,2], Gianfranco Pasut[3] & Michela Pozzobon[1,2]✉

Rhabdomyosarcoma (RMS) is a pediatric soft tissue sarcoma of mesenchymal origin with two main variants, the embryonal, less aggressive, and the alveolar RMS, more metastatic. The role of the extracellular matrix (ECM) in the growth and migration of RMS, as in other cancers, is becoming increasingly important. This work aims to study the RMS after the silencing of the proteoglycan Glypican 3, overexpressed in RMS. Using classical 2D cell culture with RMS cell lines and 3D hyaluronic acid-based hydrogel, the involvement of Glypican 3 in adhesion, proliferation, matrix degradation, and consequent cell motility was demonstrated. Functional assays were performed with the antineoplastic drug doxurubicin and the WNT3a inhibitor, ipafricept. Both in 2D and in 3D model, cell motility and proliferation were significantly impaired after Glypican 3 silencing and inhibition of the proteoglycan releasing the sulfatase enzyme SULF2. When the in vivo cell-ECM interactions were mimicked in the hyaluronic acid-based hydrogel, Doxorubicin and ipraficept were particularly effective against the GPC3-silenced RMS cells. This study lay the fundation for a different therapeutic approach against pediatric RMS that aim to dysregulate the protein microenvironment not only beat the cancer cells.

Keywords Extracellular matrix, Glypican 3, Rhabdomyosarcoma, HA-hydrogel model

Cancer cells are considered to be the key drivers of tumor progression, although in recent years the surrounding cell microenvironment has been identified as the milieu that nourishes and promotes the malignant growth[1,2]. In addition, tumor microenvironment proteins and chemokines represent a more stable therapeutic target, free from the genomic instability that characterizes cancer cells[3,4].

Rhabdomyosarcoma (RMS) is the most common soft tissue sarcoma in children, with an incidence of 4.5 cases per millions of children and adolescents. RMS develops from rhabdomyoblasts: immature myogenic mesenchymal cells committed to skeletal muscle differentiation[5–8]. RMS can be divided into two subtypes: the alveolar subtype (ARMS), which is more aggressive and metastatic, accounting for 25% of cases, and the embryonal subtype (ERMS), which is less aggressive and more localised, accounting for the remaining 75% of cases[7,9,10]. Nonetheless, approximately 20–25% of RMS cases have metastasis at diagnosis, particularly in the lung and bone marrow where the microenvironment contributes significantly to the growth potential of cancer cells. Recent studies on the extracellular matrix (ECM) support the important role of the cross-talk between transformed cells and their niche, linking ECM composition to pathological conditions. The ECM supports the growth and survival of the malignant cells and contributes to tumor dissemination. The ECM is composed by a proteoglycans (PGs) mesh, the glycocalyx, and basal membrane proteins, including collagen and fibronectin. The PG component of the ECM plays a central role in the complex events of organ development and stemness, influencing processes such as membrane receptor trafficking (during endocytosis), ligand secretion and the distribution of signaling gradients, which also significantly favour tumor development and progression. Among the PG components, Glypican 3 (GPC3) is particularly overexpressed in RMS cells, suggesting that it may be of special importance for RMS biology. GPC3 encodes a cell surface protein that is time- and tissue-restricted. It contributes to the regulation of cell growth and differentiation in a tissue-dependent manner. GPC3 has been detected in both embryonic and fetal normal tissues, as well as in several childhood and adult tumors, both sarcomas and carcinomas[11,12]. The ability of GPC3 to bind growth factors involved in tumor development and survival is due to the sulphation of its saccharide residues[13–16]. In particular, sulfatase enzyme-2 (SULF-2) modulates tumor growth by desulfating GPC3, thereby facilitating the release of bound growth factors into

[1]Department of Women's and Children's Health, University of Padova, via Giustiniani 3, Padova 35129, Italy. [2]Institute of Pediatric Research Città della Speranza, Corso Stati Uniti 4, Padova 35127, Italy. [3]Department of Pharmaceutical and Pharmacological Sciences, University of Padova, Via Marzolo 5, Padova 35131, Italy. ✉email: michela.pozzobon@unipd.it

the extracellular matrix, triggering the activity of cell surface cognate receptors and downstream intracellular cancer signaling[17].

This has been shown in hepatocellular carcinoma (HCC), where SULF-2 is overexpressed and GPC3 is abundantly desulphated, leading to the release of FGF2 or Wnt3a factors[18,19]. Indeed, SULF-2 knockdown reduces HCC cell proliferation and migration, as downregulation of GPC3 expression results in impaired FGF2 and Wnt3a binding, inhibiting oncogenic signaling related, also, to cell proliferation[18].

Consistent with its overexpression in HCC cells, GPC3 has recently been exploited as a novel tumor-associated antigen, capable of inducing both antibody-dependent cellular cytotoxicity and T cell-mediated tumor rejection in xenografts, as well as CD8 + T-cell responses in HCC patients[20].

In the case of RMS, it has been discovered the presence of redundant autocrine and paracrine circuits such as FGF signaling where deregulation of Wnt and Sonic Hedgehog, important factors for cell proliferation, have been involved in disease onset and spreading[21–23].

Based on these premises, the aim of this study was to investigate the role of the peptidoglycan GPC3 in RMS tumor growth, progression and drug response. Classic 2D and a 3D hydrogel-based cell culture models were used to characterize cell behaviour when the microenvironment was targeted with GPC3 silencing and when cells were exposed to the chemotherapeutic drugs doxorubicin[24,25] and ipafricept, a Wnt3a inhibitor[26].

Materials and methods

Cell lines

The cell lines RH30 and RH4 for the ARMS subtype, and RD and RH36 for the ERMS subtype were provided by the laboratory of Prof Gianni Bisogno, coordinator of the European Paediatric Soft Tissue Sarcoma Study Group (EpSSG). All cell lines were cultured with DMEM High Glucose (Dulbecco's modified eagle's medium: D1145-500 mL, Sigma-Aldrich, UK), 10% Fetal Bovine Serum (10270-106, Gibco, UK), 1% Pen-Strep (Penicillin and Streptomycin: 15140-122, Gibco, USA), 1% glutamine (25030-081, Gibco, UK), at 37 °C and 5% CO_2. All cell lines have already been characterized by the laboratory through specific markers, such as myogenin[6].

GPC3 silencing

The cells were plated in 24 wells, and the silencing mix was added to each well.

To the complete medium, a pool of 3 target-specific siRNA against GPC3 10 μM (sc-40640, Santa Cruz Biotechnology, USA), together with Lipofectamine (13778075, Invitrogen, Lithuania) was added. The silencing procedure was followed twice within 24 h of each other, to achieve very low levels of GPC3 expression. Cells were also treated with scramble-siRNA (sc-37007, Santa Cruz Biotechnology, USA) to prove the absence of toxicity of the treatment. After silencing, cells were treated with the SULF-2 inhibitor OKN-007 (SML2163, Sigma Aldrich, UK). The treatment lasts for 48 h at a concentration of 50 μM[27].

Doxorubicin (DOXO) (296, 21 CEC PX Pharm Ltd, UK) was added at a concentration of 1 μM for 24 h, while ipafricept at a concentration of 2 μg/ml (HY-P99667, MedChemExpress, USA) for 48 h[28,29].

Cell viability was evaluated with PrestoBlue HS cell viability reagent (P50200, Invitrogen, US) by measuring the fluorescence with Spark Tecan.

Wound healing assay

Once the gene for GPC3 was silenced, the wound-healing assay was done. In 24 wells the insert of IBIDI (81176, IBIDI, Germany) has been added in the middle. On the left and the right of the insert 30,000 cells have been seeded and 24 h later the insert was taken off. The images were taken with the optical microscope (Olympus optical co. IX71, Japan), at 0 and 24 h from the insert take off, and data were analyzed with ImageJ, using the Threshold tool.

Adhesion test

WT and siRNA-treated cells were seeded in a fibronectin-coated plate diluted 1:1000 in PBS (Fibronectin bovine plasma, F1141-1MG, Sigma-Aldrich, UK). After incubation for two hours at 37 °C, adhered cells were fixed in PFA 4%, labeled with Hoechst (Hoechst 33342, H3570, Life Technologies, USA), and analyzed with the fluorescence microscope.

Cell cycle analysis

The staining solution consisted of PBS containing Triton X-100 (0.1%; Fluka, Switzerland), DNAse-free RNAse A (0.2 mg/ml; Sigma-Aldrich, St Louis, MO, USA), and propidium iodide (1 mg/ml; Sigma-Aldrich, USA). After resuspension in cold PBS and ethanol, tubes were stored at −20 °C for at least 24 h. After staining with 300 μl/10^6 cells of staining solution, cells were analyzed.

Immunofluorescence

Immunofluorescence analysis was performed following an already published protocol[6]. For cell permeabilization, 0.05% Triton-X-100 (1610407, Bio-Rad, USA) was used. Horse Serum (16050-130, Gibco, New Zealand) was added. The primary antibody was diluted in PBS +1% Bovine Serum Albumin (A7906-100G, Sigma-Aldrich, USA) according to the dilution in Table 1. For staining, the hydrogel was incubated for 24 h with the primary antibody and then for 2 hours with the secondary antibody. Hoechst was added to allow for nuclei staining. Fluorescence microscope (DMI600B, Leica, USA) was used.

Zymography

Cells were seeded in serum-free DMEM-HG, 1% Pen/Strep, and 1% L-Gln. The serum-free conditioned medium was harvested after 24 h for zymography[30].

Target	Host	Dilution	Incubation	Product code	Producer
GPC3	rabbit	1:50	4 °C, overnight	PA5-13360	Thermo Scientific, UK
Ki67	rabbit	1:100	4 °C, overnight	15,580	Abcam, UK
GPC3	mouse	1:50	4 °C, overnight	GT2473	GeneTex, USA
GPC5	mouse	1:50	4 °C, overnight	sc-390,838	Santa Cruz Biotechnology, USA
SULF2	mouse	1:200	37 °C, 1 h	GTX38989	GeneTex, USA
ITGα9β1	mouse	1:100	4 °C, overnight	ab27947	Abcam, UK
FGF2	rabbit	1:100	37 °C, 1 h	ab208687	Abcam, UK
Fibronectin	mouse	1:100	4 °C, overnight	MA5-11981	Invitrogen, US
Anti-Vimentin	rabbit	1.100	4 °C, 24 h	ab92547	Abcam, UK
cCaspase 3	rabbit	1:200	4 °C, overnight	D175	Cell signaling technologies, USA
Anti-Rb	chicken	1:200	1 h	A21442	Invitrogen, US
Anti-mouse	goat	1:200	1 h	A11001	Invitrogen, US
Anti-Rb	chicken	1:200	1 h	A21441	Invitrogen, US
Anti-mouse	goat	1:200	1 h	A11005	Invitrogen, US

Table 1. Antibody list.

The resolving gel was made of sterile H_2O, 1.5 M Tris·HCl pH 8.8 (489973, Carlo Erba Reagents, Italy), 10% sodium dodecyl sulfate (1610301, Bio-Rad, USA), acrylamide/bis 29:1 (1610156, Bio-Rad, USA), 1% gelatin (94804, Bio-Rad, USA), 10% ammonium persulfate (A3678, Sigma-Aldrich, USA), N'-N'-N'-N' tetramethylethylenediamine (TEMED) (1610801, Bio-Rad, USA).

The stacking gel was made of sterile H_2O, 0.5 M Tris·HCl pH 6.8, 10% sodium dodecyl sulfate, acrylamide/bis 29:1, 10% ammonium persulfate, TEMED.

Working running buffer 1× was made of Tris-base, Glycine (1610718, Bio-Rad, USA), sodium dodecyl sulfate, and sterile H_2O. For sample normalization the BCA Protein Assay Kit (23227, Thermo Fisher, USA) was used. Each sample was resuspended in 5× sample buffer, made of 0.313 M Tris-HCl pH 6,8, 10% sodium dodecyl sulfate, 50% glycerol (G5516, Sigma-Aldrich, USA), 0.05% bromophenol blue (114391, Sigma-Aldrich, USA). Samples were loaded into the gel and run at 110 V and 30 mA/gel, using the marker Amersham ECL Rainbow Marker – full range (GERPN800E, Sigma-Aldrich, USA). The washing buffer was composed of Triton-X-100 (1610407, Bio-Rad, USA) and sterile H_2O in a ratio of 1:39. The incubation was run for 20 h at 37 °C with the development buffer containing 500 mM Tris pH 7.4, 100 mM $CaCl_2$ (43381, Carlo Erba Reagents, Italy), 0.2% NaN_3 (478484, Carlo Erba Reagents, Italy), H_2O sterile. The staining solution used has the following composition: Coomassie bright blue R-250 (1610400, Bio-Rad, USA), acetic acid, ethanol, and sterile H_2O. The de-staining buffer was made of ethanol, acetic acid, and H_2O. The quantification was made by the iBright (iBright 1500, Invitrogen, USA).

qRT-PCR

RNA extraction has been performed using Trizol Reagent (15596018, Life Technologies, USA). Chloroform (438613, Carlo Erba, Italy) was added. Samples of RNA: isopropanol (278475–1 L, Sigma-Aldrich, USA) 1:1 were centrifuged at 4 °C for 10 min, the supernatant of isopropanol was eliminated, and 75% ethanol (32221–2.5 L-M, Sigma-Aldrich, USA) was added. The samples were centrifuged for 10 min, and the pellets were resuspended in RNA-free water (129115, Nuclease Free-Water, Qiagen, Germany). RNA quantification was done at Nanodrop (Nanodrop 2000 spectrophotometer, Thermo Scientific, Lithuania). For reverse transcription, the high-capacity cDNA reverse transcription kit (4,368,814, Applied Biosystems by Thermo Fisher Scientific, UK) was used.

The housekeeping gene used was GAPDH; different genes were analyzed (Table 2).

SYBR green (4367659, applied biosystems by Thermo Fisher Scientific, UK) was added to detect the samples. 7500 Fast Real-Time PCR System (Applied Biosystems, USA) was used. The data were represented as a function of the threshold cycle, according to the formula $2^{-\Delta\Delta Ct}$.

Gelation of hydrogel

The cells of different cell lines were embedded into the hydrogel.

HA and HA-based hydrogel were synthesized as already described by Saggioro et al.[6]. Briefly, for the synthesis of the polymer, HA 200 kDa (Fidia Farmaceutici, Abano Terme, Italy) was dissolved in anhydrous dimethyl sulfoxide (DMSO) together with methanesulphonic acid (Merk, Darmstadt, Germany). After dissolution, 1,1-carbonyldiimidazole (Merk, Darmstadt, Germany) and, after 1 h, 2-(2-pyridyldithio) ethylamine hydrochloride (SPDC) were added. The mixture was left to react overnight under stirring at 40 °C. The obtained HA-SPDC intermediate was recovered through precipitation in ethanol and washed with EtOH/H_2O solutions at a decreasing percentage of ethanol. After solubilization in 0.5 M NaOH, and neutralization with HCl 0.5 M, the polymer was dialyzed against 0.1 M acetate buffer at pH 5 for 48 h and then against water for 24 h. The solution was lyophilized. Finally, HA-SPDC was reacted with DTT in 50 mM phosphate buffer with 2 mM EDTA at pH 7 for 1 h. The solution was dialyzed against the same buffer for 24 h and then against 1 mM EDTA for 48 h under nitrogen flow. The product was then lyophilized, and the amount of sulfhydryl groups was determined by Ellman's assay and ^{1}H-NMR.

Gene	Sequence	Accession number	Amplicon size (pb)
GAPDH	Fw. CCTCTGACTTCAACAGCGA Rev. GGTCTTACTCCTTGGAGGC	NM_001256799.3	165
GPC3	Fw. CCAAAAGAGAGGAAGGAATGG Rev. CTCAGGAGCTGGTTAATGTGC	NM_004484.4	123
GPC5	Fw. TGAAGCATGTTGTTCAGTTGTT Rev. GAAGTTCATATCATCTGGCATCC	NM_004466.6	200
SULF2	Fw. ACTCGAAACATGGACCTGGG Rev. CCCACAGTTGTCCCAGTGAT	XM_054323703.1	121
COL1α1	Fw. GCTGGAAAAGATGGTCGCAC Rev. TAACCACCACCGCTTACACC	NM_000089.4	140
CXCR4	Fw. CTTCAGTTTGTTGGCTGCGG Rev. GAAGTGTATATACTGATCCCCTCCA	NM_003467.2	119
ITGα9β1	Fw. TCAGCTTCCATGGCAAACAC Rev. AGCTTCTCTGTGACCTGACC	NM_002207.3	145
Wnt3 A	Fw. CTTTGCAGTGACACGCTCAT Rev. AGACACCATCCCACCAAACT	AB060284.1	136

Table 2. List of primers used.

For hydrogel gelation, HA-SH was resuspended in the culture medium at a final concentration of 1% [w/v] by gentle pipetting. Pellets of 2×10^5 cells were resuspended in culture medium/HA-SH solution and transferred on a glass flat bottom 96 well plate. This solution mixture was finally crosslinked with 10 kDa PEG-dimaleimide (Iris Biotech GMBH, Marktredwitz, Germany) to obtain the hydrogel. The ratio of maleimide and thiol groups was stoichiometrically kept at 1:1. Fibronectin bovine plasma (F1141-1MG, 100 µg/ml, Sigma, USA), collagen I from rat tail (ALX-522-435-0100, 600 µg/ml, Enzo Biochem, USA), and 5% of Matrigel Matrix Basement Membrane (356234, Corning, USA) were added to the gel, to create a more like in vivo model.

Then the viability was evaluated with the kit live&dead (L3224, LIVE/DEAD viability/cytotoxicity kit, Thermo Fisher scientifics, USA).

Scanning electron microscopy

For scanning electron microscopy (SEM), samples were lyophilized before imaging with a CamScan MX3000 scanning electron microscope.

Statistical analysis

For each analysis, at least five random pictures were used for data output. All graphs displayed were produced with GraphPad software 10.0.

Data were expressed as means ± SD. Four replicates for each experiment and 4 different experiments were performed for each type of analysis. For all experiments (qPCR and tissue analysis), statistical significance was determined using or an equal-variance Student's t-test or Mann–Whitney U test to compare two groups, or Anova analysis for multiple comparisons with Tukey's post hoc test. Statistical significance was determined using GraphPad 10.0 software with an equal-variance Mann-Whitney test to compare the two groups. A p-value below 0.05 was considered statistically significant.

Results

GPC3 silencing impairs RMS cells lines proliferation without affecting GPC5 expression

All the RMS cell lines used in this study exhibited elevated expression of the proteoglycan GPC3, which following silencing was significantly reduced (Fig. S1). Non-specific GPC3 silencing-related toxicity was not observed under these conditions (Fig. 1A), as increased staining of cleaved Caspase 3 (cCAS3) was only detected in a few sparse dying cells (Fig. S2D). The expression levels of proteins, (GPC5, SULF2, Ki67) related to GPC3 were assessed by immunofluorescence before and after silencing (Fig. 1A).

As illustrated in Fig. 1B and C, the expression of GPC3 protein and its family member GPC5 were examined. GPC5 expression was assessed due to the high homology with GPC3, which could substitute for GPC3 after silencing. However, GPC5 exhibited consistent expression in all the cell lines following GPC3 silencing, further increasing in RH4 ARMS cells seemingly compensating for the absence of GPC3 (Fig. 1C). In contrast, the proliferation marker Ki67 (Fig. 1B and C) decreased after treatment, supporting the hypothesis that GPC3 is somehow involved in RMS cell proliferation.

Finally, the expression of SULF2, the enzyme that activates GPC3, remained unchanged, except in RH30 cells, where overexpression of SULF2 may help to restore GPC3, which is particularly important for the dissemination of ARMS cells.

Adhesion and migration are greatly decreased after silencing GPC3 in both ARMS and ERMS

Evaluation of GPC3 expression at early time points of silencing revealed the persistent absence of protein in the cell lines, except for RH36 cells (Fig. 2A). This finding led to investigate the involved biological processes, including adhesion and migration, in which GPC3 plays a role. As depict in Fig. 2B, the counts of cells per area were examined in the presence and absence of fibronectin, highlighting the intrinsic inability of silenced cells

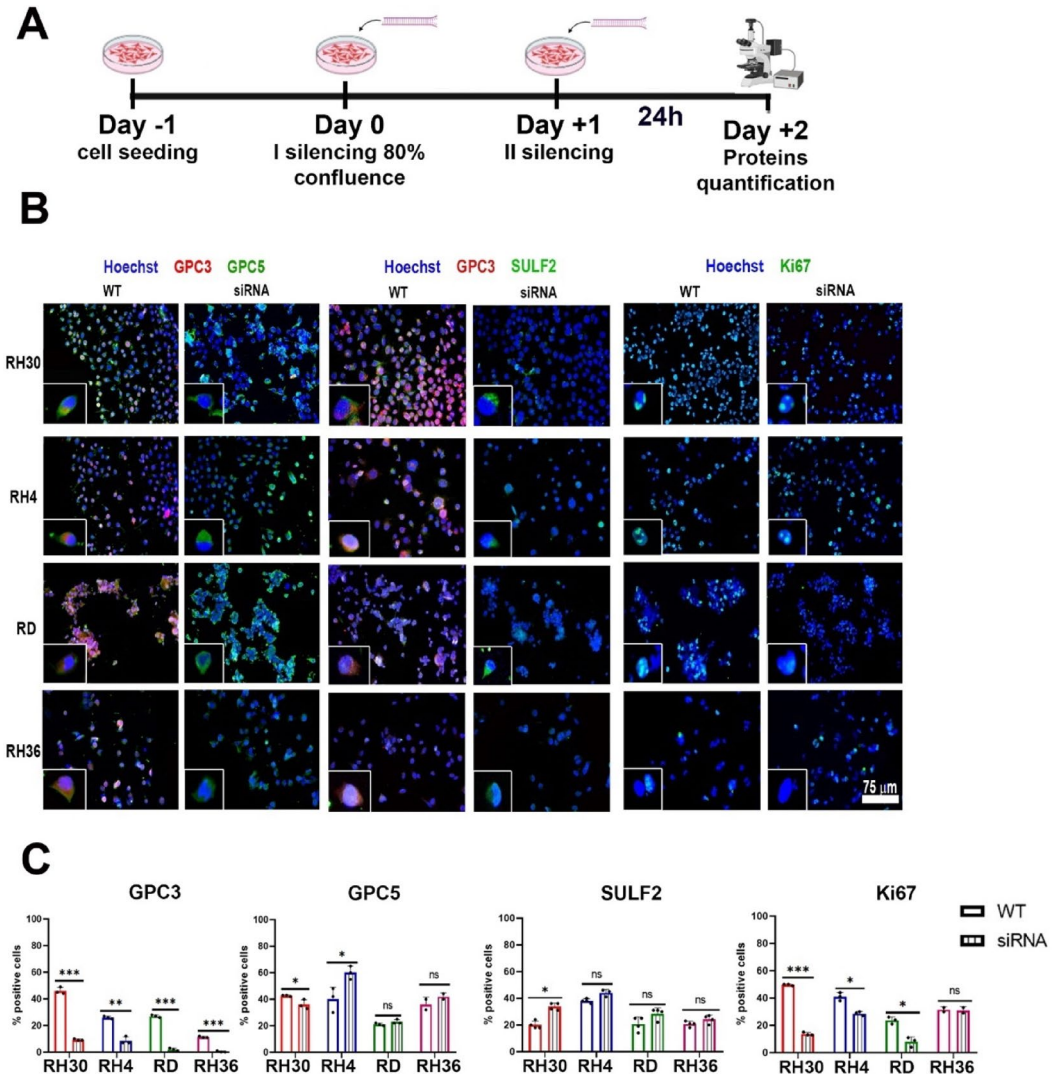

Fig. 1. GPC3 silencing. **(A).** Cartoon illustrating the experimental protocol. Two siRNA treatments were performed after cell seeding. Analysis was performed 24 h after the second treatment. (**B**). Protein expression levels in wild-type (WT) and siRNA-treated cells. (**C**). Analysis of protein expression. GPC3 expression is reduced by siRNA treatment, with the treatment being highly specific while not affecting GPC5 expression. After silencing, reduced cell proliferation (Ki67 expression) is also observed. SULF2 expression increased possibly to restore the balance of proteoglycan expression. (Mann-Whitney test; *: $p < 0.05$; **: $p < 0.01$; ***: $p < 0.001$). $N = 4$ experiments. In each experiment 4 replicates per each condition.

to rapidly adhere to the fibronectin coating. These results confirmed the primary role of GPC3 in cell adhesion, particularly for the ARMS RH30 cell line.

Transwell migration and wound-healing assays were performed to quantitatively assess GPC3 expression in cell migration. As expected, all GPC3-silenced RMS cells showed a significant decrease in transwell migration compared to GPC3-expressing cells (Fig. 2C-E). Remarkably, these observations were also evident in the wound healing assay. While, no clear difference was observed between ARMS and ERMS cell migration, a clear distinction was noted between treated and untreated cells for each cell line (Fig. 2D and E). Based on these other findings, it can be hypothesized that GPC3 may play a role in regulating the metastatic behaviour of RMS cells.

SULF2 inhibition directly influences RMS cell growth

In order to avoid the continuous SULF2 activity following GPC3 silencing, we decided to directly inhibit the enzyme itself. We aimed to analyze both GPC3 and SULF2 protein expression in these setting, in addition to the secreted protein delivered by SULF2, FGF2. We confirmed that after the addition of the SULF2 inhibitor, GPC3 availability was greatly reduced in parental cells and completely lost in GPC3-silenced ones, together with a significant downregulation of GPC5 (Fig. 3). The paramount role of the SULF2 in the activation of GPC3 was proven. However, in the presence of the enzyme inhibitor factor, a FGF2 overproduction was observed, with the exception of RH4 cells (Fig. 3B and S2B). With regard to ECM protein secretion, the inhibition of SULF-2 did not affect fibronectin synthesis, but it did cause an marked alteration in cell proliferation and the cell cycle

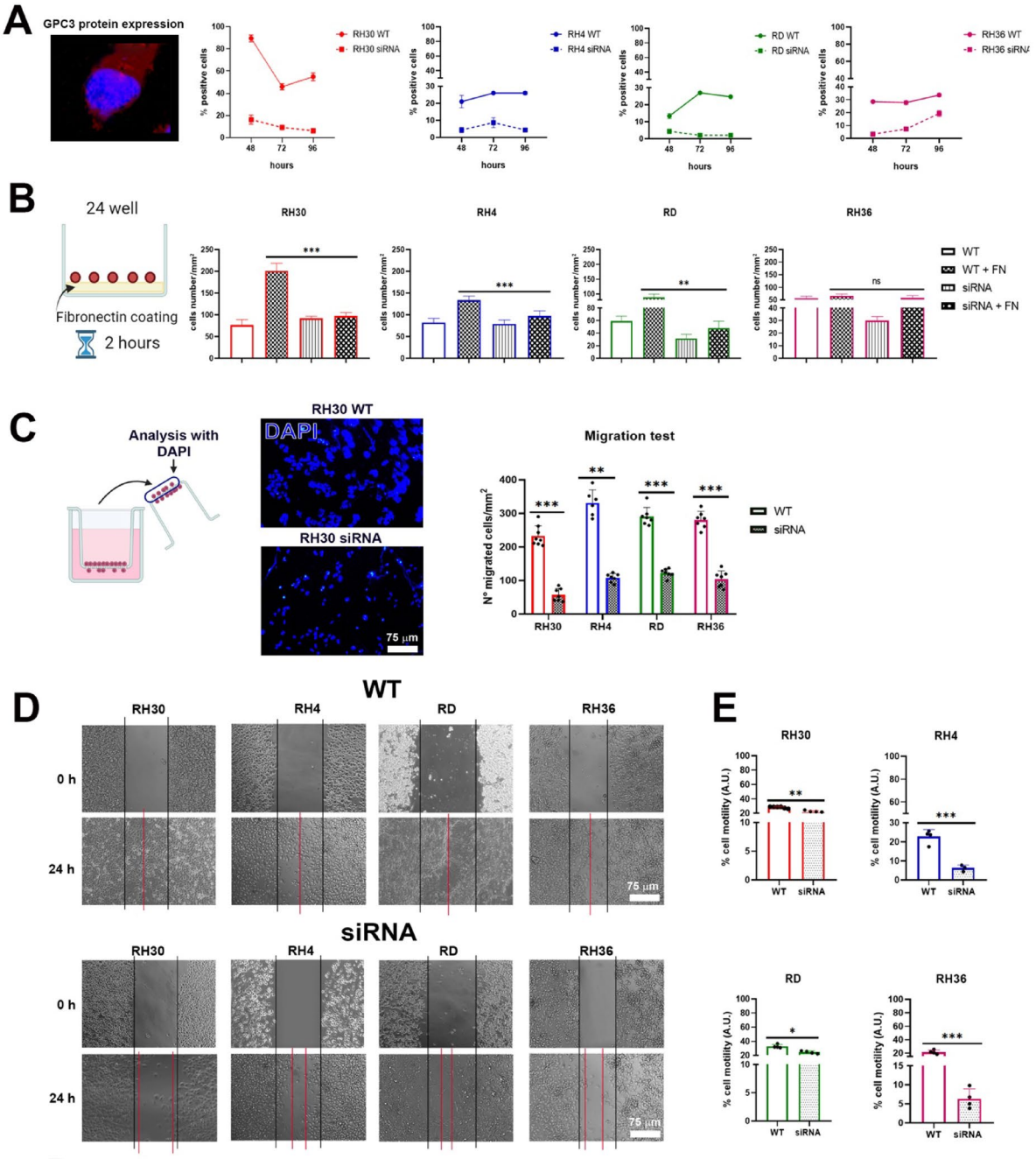

Fig. 2. GPC3 expression over time and adhesion assay and cell migration. **(A).** GPC3 expression at different time points following a second siRNA treatment. The GPC3 expression in siRNA-treated cells was consistently lower compared to wild-type (WT) cells, even after 96 h of treatment. (**B).** Adhesion assay analysis reveal that WT cells exhibit superior adhesion compared to siRNA-treated cells in the presence of a fibronectin (FN) coating. **(C).** Gross appearance of the cells in the migration assay of WT and siRNA treated cells. Scale bar 75 µm. Quantification of the migrated cells. Treated cells did not migrate through the transwell like WT cell. **(D).** Gross appearance of the cells in the wound healing assay with WT cells *and* with siRNA treated cells. WT cells closed the wound *while* siRNA treated cells did not, in particular the ARMS cell line RH30. **(E).** Quantification of the wound healing assay. (Mann-Whitney test; **: $p < 0.01$; ***: $p < 0.001$). $N = 4$ experiments. In each experiment 4 replicates per each condition.

(Fig. 3C).Vimentin, a protein that is involved in maintaining cell structure, significantly changed in expression after silencing (Fig. S2 C). In contrast, the levels of all the proteins described above were reduced when SULF2 enzyme activity was inhibited together with GPC3 silencing (Fig. 3C right). This effect was also observed for the proteins involved in ECM composition (Col1α1, GPC3, GPC5, SULF2) and cell migration (CXCR4) (Fig. S3). GPC3 gene expression decreased after the treatments, while SULF2 increased, indicating an attempt to

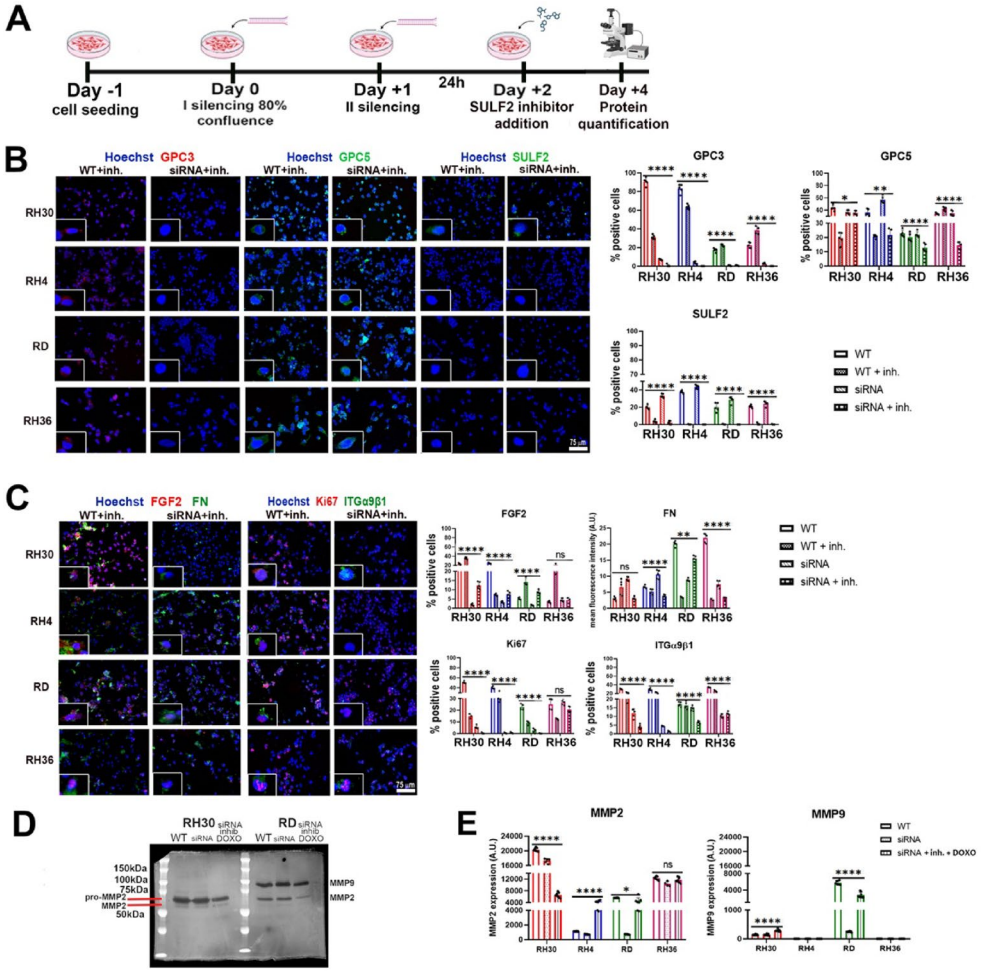

Fig. 3. SULF2 inhibition directly influences RMS cell growth and extracellular matrix proteins. **(A).** Cartoon of the experiment. **(B).** *Left.* Protein expression in WT cells and siRNA-treated cells, after SULF2-inhibitor treatment. Scale bar 75 µm. *Right.* After the SULF2-inhibitor treatment, the GPC3 expression was lower, and completely absent after siRNA + SULF2 treatments. GPC5 expression was significantly decreased after the addition of SULF2-inhibitor to the silenced cells. **(C).** *Left.* Protein expression in WT cells and siRNA-treated cells, after SULF2-inhibitor treatment. *Right.* FGF2 expression, which is bound to the GPC3 core protein, decreased in parallel with GPC3 expression. FN expression, which is produced by tumor cells, decreased after treatment. Cell proliferation was further diminished after treatment with the SULF2 inhibitor. ITGα9β1 expression decreased, indicating a reduced ability of cells to enter the cell cycle in a new metastatic process/niche. (**D).** Example of zymography gel of RH30 and RD wild type and siRNA cell line. (**E).** Quantification of the most abundant MMPs in RMS cells under different conditions (MMP2 = pro-MMP2 + MMP2; Tukey's post hoc test; *: $p < 0.05$; ****: $p < 0.0001$). $N = 4$ experiments. In each experiment 4 replicates per each condition. For zymograghy: 4 technical replicates, 2 different experiments for RH4 and RH36, 3 for RH30 and RD (see supplementary).

synthesise new SULF2 protein with consequent activation of additional GPC3. Conversely, the GPC5 gene was not detected, and the protein was found to be highly present. The CXCR4 gene demonstrated no alterations in response to the combination of DOXO, SULF2-inhibitor and GPC3 siRNA, whereas Col1α1 expression was reduced in cells subjected to triple treatment, suggesting a potential suppression of matrix formation. The expression of the proliferation markers Ki67 and Wnt3a also decreased after GPC3 silencing, as did ITGα9β1 protein, a factor known to be involved cell cycle reactivation (Fig. 3C and S2 A). Tumor migration appeared to be directly linked to the microenvironmental proteins that determine the shape and mechanical properties of the surrounding ECM. Therefore, we focused on understanding the ECM dysregulation properties after GPC3 silencing, SULF2 inhibition, and DOXO addition by assessing the expression of MMPs (gelatinases), enzymes that are involved in microenvironment remodeling. In these conditions, the expression of active MMP2 (67 kDa) was found to decrease in the RH30 cell line following the triple treatment (Fig. 3D, E), while its expression increased in the RH4 and RD cell lines. In ARMS, MMP9 (82 kDa), which exhibits lower expression levels compared to MMP2, demonstrated an increase in response to treatment (Fig. 3D and E). In ERMS cells, MMP9, which is present in the untreated control, decreased only after silencing, while with the combination of GPC3

siRNA, SULF2 inhibitor and DOXO it regained expression (Fig. 3E and S8). These results highlight how ECM remodelling is influenced by the proteoglycan GPC3.

Microenvironment dysregulation and drug-targeting tumor cells induce cell death

To evaluate the combined effect of microenvironmental impairment subsequent to GPC3 silencing and the administration of anti-cancer proliferation drugs, the expression of Ki67 and cleaved caspase 3 (cCAS3) proteins was assessed. The use of DOXO following silencing was demonstrated to affect the cell viability (Fig. S4). Furthermore, the triple treatment with GPC3 siRNA, SULF2-inhibitor and DOXO, as shown in Fig. 4A, resulted in a significant impairment in cell proliferation, resulting in up to 15% of cell death (Fig. 4A and B). When it was given in preference of DOXO, the cells reached a steady state in which proliferation was blocked (Fig. 4B and C). The metabolic activity of the cells was strongly impaired when ipafricept was added (Fig. 4D), most likely due to perturbations in the S phase of RMS cells (Fig. S5, RH30). As expected, the combined treatment was more effective in all RMS cells.

Migration and proliferation in the 3D hydrogel are significantly different from the 2D cell culture

The HA-based hydrogels have previously been shown to be a promising environment that well recapitulates the in vivo conditions of RMS, in particular after the analysis of the extracellular matrix proteins. Indeed, as already shown by our group, fibronectin and collagen play a paramount role in recapitulating the RMS surrounding in our hydrogel[6].

Here, the presence of RMS RH30 and RD cells was detected in the hydrogel by means of SEM. The shape of the cells, whether elongated or round, was found to correlate with the presence or absence of GPC3 (Fig. 5A and

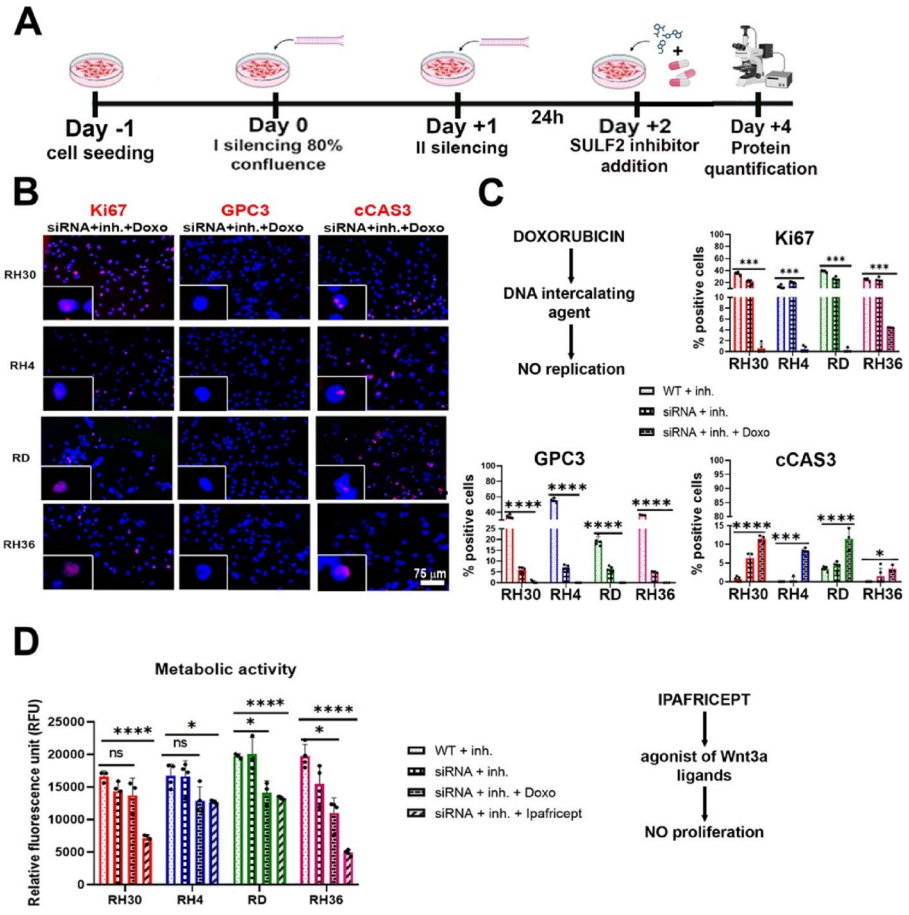

Fig. 4. Effects of silencing, SULF-2 inhibitor and drugs on cell proliferation, death, and metabolic activity. **(A).** Cartoon of the experiment. After cell seeding, two siRNA treatments were performed to obtain a lower value of GPC3, followed by SULF2 inhibitor treatment and DOXO administration. (**B**). Immunofluorescence. Protein expression in siRNA + SULF2-inhibitor + DOXO treated cells. Scale bar: 75 µm. (**C).** As can be seen in the graphs, Ki67, and GPC3 decrease in treated cells, while death cells (cleaved Cas3 expression) increase. (**D).** Metabolic activity under different conditions showed that the viability decreased in DOXO-treated cells, and further in ipafricept-treated cells. (Tukey's post hoc test; *: $p < 0.05$; ***: $p < 0.001$, ****: $p < 0.0001$). $N = 4$ experiments. In each experiment 4 replicates per each condition.

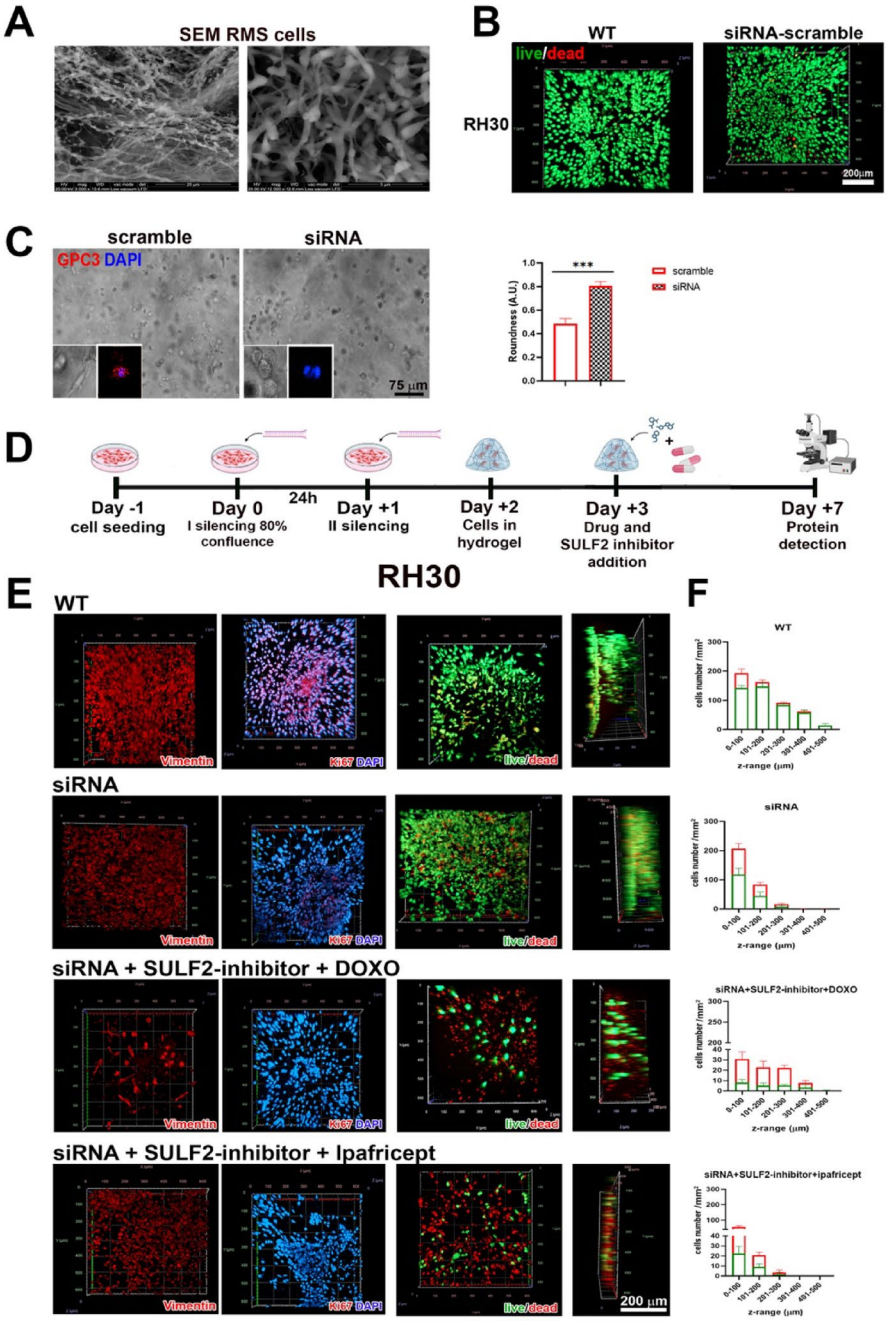

Fig. 5. First characterization of cells in hydrogel and their 3D distribution after SULF-2 inhibition and drug addition. **(A)**. SEM of hydrogel with cells. Scale bar: 20 µm and 5 µm. **(B).** Live and dead assay of RMS cells in the hydrogel also after scramble treatment (RH30 cell line as example). **(C).** RMS cells in hydrogel after scramble and siRNA treatment; roundeness evaluation. Scale bar: 75 mm Scale bar: 200 µm. **(D).** Cartoon of the hydrogel seeding procedure with drug and SULF-2 inhibition. **(E).** *First row.* WT cells have better migration, viability, and proliferation than other conditions. *Second row.* The addition of siRNA against GPC3 decreased cell mobility and proliferation, *Third and forth row.* While the addition of SULF2-inhibitor and drugs strongly decreased cell proliferation and distribution, indicating a key role of GPC3 in the above mentioned functions. Scale bar: 200 µm. **(F).** Histograms of the different cell condition showing cell distribution calculated as the number of cells per volume of 10 mm^3 across the z-axis (z-range). $N = 4$ experiments per each condition. Each condition in quadriplicate.

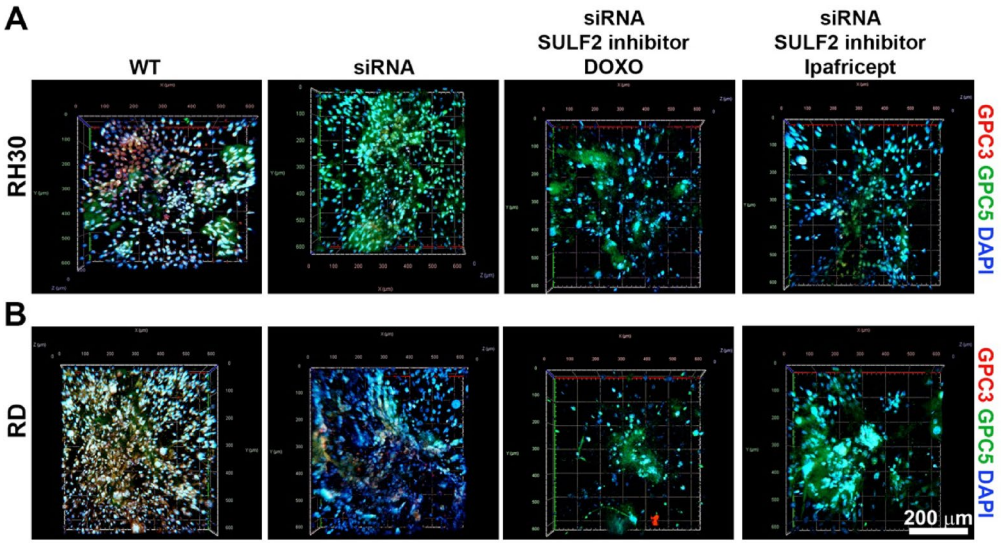

Fig. 6. Evaluation of GPC3 and GPC5 expression in GPC3-silenced RH30 (ARMS cells) and RD (ERMS cells) exposed to SULF2 inhibitor and DOXO or SULF2 inhibitor and Ipafricept. (**A**). RH30 cells in 3 different experimental conditions. GPC3 expression (red signal) decreases in treated cells, while GPC5 (green signal) does not under the same experimental conditions. (**B**). RD cells in 3 different experimental conditions. GPC3 expression (red signal) decreases in treated cells, while GPC5 (green signal) does not under the same experimental conditions. $N = 4$ experiments per each condition. Each condition in quadruplicate.

B). Furthermore, the high level of cell viability observed after administration of scramble GPC3 siRNA provided further evidence that transfection per se was not toxic (Fig. 5B and C; Fig. S6).

It is important to note that untreated RMS cells (WT) spread homogeneously on the hydrogel support, whereas GPC3 silenced cells confirmed their impaired motility, at least in part due to the higher percentage of cell death (Fig. 5E).

The addition of SULF2 inhibitor and DOXO further impaired RMS cell migration on the hydrogel, but also affected cell proliferation and viability (Fig. 5D-F). A more pronounced effect was observed in the presence of ipafricept, both in ARMS (RH30) and ERMS (RD) cells (Fig. 5D and S7).

In the 3D model, the presence of GPC5 did not protect and rescue the GPC3-silenced cells, demonstrating for the first time, that the presence of GPC3 is essential for RMS cell migration and survival (Fig. 6).

Discussion

In the present study we demonstrated for the first time that an ECM protein, such as the proteoglycan GPC3, is of paramount importance for the migration and proliferation of RMS cancer cells.

Malignant cells do not act alone in cancer progression but require sustained interactions and crosstalk with supporting cells and ECM components that form the tumor microenvironment[1,2,16]. Soluble molecules of the ECM, present in proximity of tumor cells, bind to membrane receptors and initiate intracellular signaling cascades necessary to sustain proliferation, angiogenesis, initiation of invasion and metastasis[31]. Glypicans are one of the most important matrix components that regulate the availability of biomolecules in the surrounding milieu.

Six glypicans (GPC1-6) have been described in mammals, bound to the outer surface of the plasma membrane by glycosyl-phosphatidylinositol anchors. They regulate several developmental signaling pathways, such as Wnt or Hedgehog, by acting as co-receptors and storage sites for many heparin-binding growth factors.

Glypican-3 (GPC3) is protein that is expressed in a time- and tissue-restricted manner and also expressed in pathological conditions including cancer. Following GPC3 silencing, cell proliferation, adhesion, and migration are severely impaired following GPC3 silencing, as demonstrated in RH30 alveolar rhabdomyosarcoma cells, representing the most aggressive RMS subtype known to date. It is worth noting that GPC3 is more abundant in ARMS than in ERMS cells, and this correlates with the tendency of ARMS to invade and spread widely. Indeed, all of the aforementioned biological processes were significantly downregulated in GPC3-silenced ARMS cell lines, whereas in ERMS were dependent on the specific cell line.

GPC3 silencing in RMS cells was highly specific, as the expression of the family member GPC5 appeared to be unaffected by the knockdown and even increased after treatment. GPC5 shares 63% homology with GPC3 and is also expressed in RMS cells[32,33]. However, although GPC5 is expressed during development in the kidney, testis, limbs, and brain, unlike GPC3, it also persists in the brain during adulthood. Therefore, in addition to silencing GPC3, we decided to inhibit the SULF-2 enzyme, which is shared by both GPC3 and GPC5 for their maturation and proper activation. SULF-2 has been demonstrated to promote tumor growth by releasing soluble growth factors from GPCs in the ECM, which in turn induce cell surface cognate receptor activity and downstream intracellular cancer signaling upon ligand binding. To assess the importance of GPC3 in RMS

biology and aggressiveness, we used the SULF-2 inhibitor which has been shown to inhibit cell proliferation, viability, and migration in different tumor models, and to promote cell death by increasing apoptotic caspase 3 enzyme activity[14,27]. We demonstrated that although SULF-2 was detectable after GPC3 silencing, it became undetectable after activity inhibition in all treated cell lines, negatively affecting GPC5 expression as hypothesized.

Cell adhesion is closely correlated with fibronectin production and extracellular deposition, as fibronectin is one of the major components of the ECM that controls tissue development, cancer progression, wound healing, and the development of diseases associated with fibrosis[34]. We have previously shown that RMS cancer cells produce their own ECM proteins in order to sustain their growth, including fibronectin[35]. Here, we observed that after GPC3 silencing and SULF-2 inhibition, the ECM surrounding RMS cells decreased fibronectin deposition. In addition to this, the expression of ITGα9β1, a fibronectin receptor involved in cell cycle regulation at the pre-metastatic niche[36–38], was deregulated by the combinatorial treatment, along with the disruption of cell proliferation and extracellular matrix formation.

Microenvironmental remodeling has therefore been studied following administration of DOXO, an anthracycline drug that has been extensively used in the treatment of various cancers, including rhabdomyosarcoma[39]. In vitro studies have demonstrated that anthracyclines inhibit invasion of cancer cells derived from various solid tumors. The anti-invasive effect of anthracyclines involves the downregulation of matrix metalloproteinases (MMPs), the disorganization of the cytoskeleton and the inhibition of focal adhesion kinases (FAK)[40–42]. However, under certain circumstances ECM proteins have been observed to modulate the antimigratory and apoptotic effects of chemotherapeutic drugs, thereby explaining the drug resistance and disease progression events that occur in many cases[43,44]. Among the proteins involved in ECM remodelling and degradation, MMPs are of particular importance, in both healthy and pathological conditions[45–47]. In particular, the expression of MMP2 and MMP9 has been linked to tumor growth, progression, and metastasis, and correlates with cancer aggressiveness and response to therapy[45]. Here, the reduced MMP expression following GPC3 silencing was found to be increased after SULF-2 inhibition and DOXO treatment, an effect that can be explained by the action of DOXO, which activates microRNAs involved in cell migration[46–48]. In this study, the efficacy of DOXO in combination with GPC3 silencing and the SULF-2 inhibitor was investigated. The results demonstrated that the combination therapy was effective in reducing cell proliferation while inducing cell death. However, since the metabolic activity of RMS cells was not reduced after the combinatorial treatment, an early inhibitor of RMS cell proliferation, Ipafricept, was used instead of DOXO. Indeed, Ipafricept synergized with GPC3 silencing and the SULF-2 inhibitor, and also reduced metabolic activity. Ipafricept, a recombinant fusion protein that sequesters Wnt ligands, does not act at the DNA level but blocks Wnt-dependent proliferative signaling early at the plasma membrane[29,49,50]. Finally, a proprietary hyaluronic-based hydrogel tunable with ECM proteins was utilized. This has been demonstrated to sense RMS cells to feel the spatial and mechanical interactions of the in vivo microenvironment[6]. In the hydrogel support, the RMS cells migrated in all directions, interacting with matrix-embedded fibronectin and collagen I proteins[6,51]. The 3D distribution of both viable WT and silenced cells was striking. However, the percentage of dead cells in the latter was significantly increased. The percentage of dead cells increased further after drug treatment, particularly with ipafricept, which was much more potent in RD ERMS cells.

Notably, GPC5 protein secretion persisted under these conditions, suggesting a potential for further investigation of an inhibitory strategy capable of silencing both GPC3 and GPC5.

In conclusion, we here demonstrated that GPC3 (and GPC5) plays a pivotal role in the growth, proliferation and expansion of RMS. To this end two models were developed: the first, a simple 2D model, allowed us to underline the pivotal role of GPC3 and proved to further expand the study in the second, more complex, 3D model. The latest represents the more suitable condition for future drug testing and new silencing strategies with patient-derived cells.

Data availability

The materials are already available in the manuscript. Raw data are available under reasonable request to michela.pozzobon@unipd.it.

Received: 17 December 2024; Accepted: 20 May 2025
Published online: 01 July 2025

References

1. Paolillo, M. & Schinelli, S. Extracellular matrix alterations in metastatic processes. *Int J. Mol. Sci* **20**, (2019).
2. Winkler, J., Abisoye-Ogunniyan, A., Metcalf, K. J. & Werb, Z. Concepts of extracellular matrix remodelling in tumour progression and metastasis. *Nat Commun* **11**, (2020).
3. Lian, X. et al. Defining the extracellular matrix of rhabdomyosarcoma. *Front Oncol* **11**, (2021).
4. Wang, J. J., Lei, K. F. & Han, F. Tumor microenvironment: recent advances in various cancer treatments.
5. Xiao, Y. & Yu, D. Tumor microenvironment as a therapeutic target in cancer. *Pharmacol. Ther.* **221**, 107753 (2021).
6. Saggioro, M. et al. A rhabdomyosarcoma hydrogel model to unveil cell-extracellular matrix interactions. *Biomater. Sci.* **10**, 124–137 (2022).
7. Martin-Giacalone, B. A., Weinstein, P. A., Plon, S. E. & Lupo, P. J. Pediatric rhabdomyosarcoma: epidemiology and genetic susceptibility. *J Clin. Med* **10**, (2021).
8. Rees, H. et al. *Rhabdomyosarcoma Standard Clinical Practice document 1 CLINICAL PRACTICE GUIDELINES FOR PATIENTS WITH RHABDOMYOSARCOMA Collaborators from* (Widening country Reviewers,).
9. Skapek, S. X. et al. Rhabdomyosarcoma. *Nat. Rev. Dis. Primers.* **5**, 1 (2019).
10. Hinson, A. R. P. et al. Human rhabdomyosarcoma cell lines for rhabdomyosarcoma research: utility and pitfalls. *Front Oncol* **3**, (2013).
11. Zhu, Z. W. et al. Enhanced glypican-3 expression diverentiates the majority of hepatocellular carcinomas from benign hepatic disorders. https://doi.org/10.1136/gut.48.4.558

12. Boily, G., Saikali, Z. & Sinnett, D. Methylation analysis of the glypican 3 gene in embryonal tumours. *Br. J. Cancer*. **90**, 1606–1611 (2004).
13. Rosen, S. D. & Lemjabbar-Alaoui, H. SULF-2: AN EXTRACELLULAR MODULATOR OF CELL SIGNALING AND A CANCER TARGET CANDIDATE. https://doi.org/10.1517/14728222.2010.504718
14. Hammond, E., Khurana, A., Shridhar, V. & Dredge, K. The role of heparanase and sulfatases in the modification of heparan sulfate proteoglycans within the tumour microenvironment and opportunities for novel cancer therapeutics. *Front Oncol* 4 JUL, 195 (2014).
15. Lai, J. P. et al. Sulfatase 2 Up-Regulates glypican 3, promotes fibroblast growth factor signaling, and decreases survival in hepatocellular carcinoma. (2008). https://doi.org/10.1002/hep.22202
16. Hill, K. E., Lovett, B. M. & Schwarzbauer, J. E. Heparan sulfate is necessary for the early formation of nascent fibronectin and collagen I fibrils at matrix assembly sites. *J. Biol. Chem.* **298**, 101479 (2022).
17. Lanzi, C., Zaffaroni, N. & Cassinelli, G. Targeting Heparan sulfate proteoglycans and their modifying enzymes to enhance anticancer chemotherapy efficacy and overcome drug resistance. *Curr Med. Chem* **24**, (2017).
18. Fico, A., Maina, •, F. & Dono, R. Fine-tuning of cell signaling by glypicans. *VISIONS & REFLECTIONS* https://doi.org/10.1007/s00018-007-7471-6
19. Desai, A., Sandhu, S., Lai, J. P. & Sandhu, D. S. Hepatocellular carcinoma in non-cirrhotic liver: A comprehensive review. *World J. Hepatol.* **11**, 1 (2019).
20. Ofuji, K., Saito, K., Yoshikawa, T. & Nakatsura, T. Critical analysis of the potential of targeting GPC3 in hepatocellular carcinoma. *J. Hepatocell Carcinoma*. **1–35** https://doi.org/10.2147/JHC.S48517 (2014).
21. De Giovanni, C., Landuzzi, L., Nicoletti, G., Lollini, P. L. & Nanni, P. Molecular and cellular biology of rhabdomyosarcoma. (2009). http://dx.doi.org/10.2217/fon.09.97 5, 1449–1475
22. Roma, J., Almazán-Moga, A., De Sánchez, J., Gallego, S. & Notch Wnt, and Hedgehog Pathways in Rhabdomyosarcoma: From Single Pathways to an Integrated Network. (2012). (2012).
23. Salvo, D., Raimondi, M., Vella, L., Adesso, S. & Ciarapica, L. Hyper-Activation of Notch3 amplifies the proliferative potential of rhabdomyosarcoma cells. *PLoS One*. **9**, 96238 (2014).
24. Rivankar, S. An overview of doxorubicin formulations in cancer therapy. *J. Cancer Res. Ther.* **10**, 853 (2014).
25. Meredith, A. M. & Dass, C. R. Increasing role of the cancer chemotherapeutic doxorubicin in cellular metabolism. *J. Pharm. Pharmacol.* **68**, 729–741 (2016).
26. Jimeno, A. et al. Cancer therapy: clinical A First-in-Human phase I study of the anticancer stem cell agent Ipafricept (OMP-54F28), a decoy receptor for Wnt ligands, in patients with advanced solid tumors. https://doi.org/10.1158/1078-0432.CCR-17-2157
27. Zheng, X. et al. The human sulfatase 2 inhibitor 2,4-Disulfonylphenyl-tert-Butylnitrone (OKN-007) has an antitumor effect in hepatocellular carcinoma mediated via suppression of TGFB1/ SMAD2 and Hedgehog/GLI1 signaling. *Genes Chromosomes Cancer*. **52**, 225–236 (2013).
28. Baxter-Holland, M. & Dass, C. R. Doxorubicin, mesenchymal stem cell toxicity and antitumour activity: implications for clinical use. *J. Pharm. Pharmacol.* **70**, 320–327 (2018).
29. Ipafricept (OMP-54F. 28) | Wnt Inhibitor | MedChemExpress. https://www.medchemexpress.com/ipafricept.html
30. Toth, M. & Fridman, R. Assessment of gelatinases (MMP-2 and MMP-9) by gelatin zymography. *Methods Mol. Med.* **57**, 163–174 (2001).
31. Theocharis, A. D., Skandalis, S. S. & Gialeli, C. Karamanos, N. K. Extracellular matrix structure. *Adv. Drug Deliv Rev.* **97**, 4–27 (2016).
32. Li, F., Shi, W., Capurro, M. & Filmus, J. Glypican-5 stimulates rhabdomyosarcoma cell proliferation by activating Hedgehog signaling. *J. Cell Biol.* **192**, 691–704 (2011).
33. Williamson, D. et al. Role for amplification and expression of Glypican-5 in rhabdomyosarcoma. *Cancer Res.* **67**, 57–65 (2007).
34. Ghura, H. et al. Inhibition of fibronectin accumulation suppresses TUMOR growth. *Neoplasia* **23**, 837 (2021).
35. D'Agostino, S. et al. Rhabdomyosarcoma cells produce their own extracellular matrix with minimal involvement of Cancer-Associated fibroblasts: A preliminary study. *Front Oncol* **10**, (2021).
36. Xu, S. et al. Integrin-a9b1 as a novel therapeutic target for refractory diseases: recent progress and insights. https://doi.org/10.3389/fimmu.2021.638400
37. Navarro, N. et al. Integrin alpha9 emerges as a key therapeutic target to reduce metastasis in rhabdomyosarcoma and neuroblastoma. *Cell. Mol. Life Sci.* **79**, 546 (2022).
38. Masià, A. et al. Notch-mediated induction of N-cadherin and α9-integrin confers higher invasive phenotype on rhabdomyosarcoma cells. *Br. J. Cancer*. **107**, 1374–1383 (2012).
39. Gianni Bisogno, M. et al. D. S. Addition of dose-intensified doxorubicin to standard chemotherapy for rhabdomyosarcoma (EpSSG RMS 2005): a multicentre, open-label, randomised controlled, phase 3 trial. *Lancet* **19**, 1061–1071 (2018).
40. Park, H. J. et al. Inhibitory effect of DA-125, a new anthracyclin analog antitumor agent, on the invasion of human fibrosarcoma cells by down-regulating the matrix metalloproteinases. https://doi.org/10.1016/j.bcp.2005.10.007
41. Harisi, R. et al. Repopulation of osteosarcoma cells after treatment with doxorubicin in the presence of extracellular matrix biopolymers. https://doi.org/10.1007/s00280-005-0165-6
42. Van Nimwegen, M. J., Huigsloot, M., Camier, A., Tijdens, I. B. & Van De Water, B. Focal adhesion kinase and protein kinase B cooperate to suppress Doxorubicin-Induced apoptosis of breast tumor cells. *Mol. Pharmacol.* **70**, 1330–1339 (2006).
43. Said, G. et al. Extracellular matrix proteins modulate antimigratory and apoptotic effects of Doxorubicin. *Chemother Res Pract* 1–10 (2012). (2012).
44. Shin, S. H., Choi, Y. J., Lee, H., Kim, H. S. & Seo, S. W. Oxidative stress induced by low-dose doxorubicin promotes the invasiveness of osteosarcoma cell line U2OS in vitro. *Tumour Biol.* **37**, 1591–1598 (2016).
45. Ricci, S., D'Esposito, V., Oriente, F., Formisano, P. & Di Carlo, A. Substrate-zymography: A still worthwhile method for gelatinases analysis in biological samples. *Clin. Chem. Lab. Med.* **54**, 1281–1290 (2016).
46. Beji, S. et al. Doxorubicin upregulates CXCR4 via miR-200c/ZEB1-dependent mechanism in human cardiac mesenchymal progenitor cells. *Cell Death Dis* 8, 3020 (2017).
47. Long, L., Xiang, H., Liu, J., Zhang, Z. & Sun, L. ZEB1 mediates doxorubicin (Dox) resistance and mesenchymal characteristics of hepatocarcinoma cells. *Exp. Mol. Pathol.* **106**, 116–122 (2019).
48. Regenbogen, S. et al. Cytotoxic drugs in combination with the CXCR4 antagonist AMD3100 as a potential treatment option for pediatric rhabdomyosarcoma. *Int. J. Oncol.* **57**, 289–300 (2020).
49. Le, P., Mcdermott, J. D. & Jimeno, A. Targeting the Wnt pathway in human cancers: therapeutic targeting with a focus on OMP-54F28. (2014). https://doi.org/10.1016/j.pharmthera.2014.08.005
50. Sun, Y., Wang, W. & Zhao, C. Frizzled receptors in tumors, focusing on signaling, roles, modulation mechanisms, and targeted therapies. *Oncol. Res.* **28**, 661 (2021).
51. Yoo, K. M., Murphy, S. V. & Skarda, A. A. Rapid crosslinkable Maleimide-Modified hyaluronic acid and gelatin hydrogel delivery system for regenerative applications. *Gels* **7**, 1–17 (2021).

Acknowledgements

We thanks Chiara Frasson for her valuable support in cytofluorimetric analysis.

Author contributions

M.B., S.DA. performed the experiments, data collection and interpretation, wrote the article; A.G. created the hydrogel and help with experiments; E.P., P.B. data interpretation. G.B. G.P. read and approved the article. M.P. conceived the experiments, analyzed the data, wrote and approved the article. All the authors approved the article.

Funding

This work has been supported by Project 21/07 Institute of Pediatric Research Città della Speranza. PI: Michela Pozzobon.

Declarations

Competing interests

The authors declare no competing interests.

Ethics approval and consent to partecipate

Not applicable. The present work use commercially available cell lines.

Consent for publication

All authors agree to publish the work.

Additional information

Supplementary Information The online version contains supplementary material available at https://doi.org/10.1038/s41598-025-03466-x.

Correspondence and requests for materials should be addressed to M.P.

Reprints and permissions information is available at www.nature.com/reprints.

Publisher's note Springer Nature remains neutral with regard to jurisdictional claims in published maps and institutional affiliations.